The Astrophysical Journal Letters, 911:L2 (7pp), 2021 April 10 https://doi.org/10.3847/2041-8213/abef00
© 2021. The Author(s). Published by the American Astronomical Society.
OPEN ACCESS

The Solar-cycle Variations of the Anisotropy of Taylor Scale and Correlation Scale in the Solar Wind Turbulence

G. Zhou[1,2] and H.-Q. He[1,3,4]
[1] Key Laboratory of Earth and Planetary Physics, Institute of Geology and Geophysics, Chinese Academy of Sciences, Beijing 100029, People's Republic of China; hqhe@mail.iggcas.ac.cn
[2] College of Earth and Planetary Sciences, University of Chinese Academy of Sciences, Beijing 100049, People's Republic of China
[3] Innovation Academy for Earth Science, Chinese Academy of Sciences, Beijing 100029, People's Republic of China
[4] Beijing National Observatory of Space Environment, Institute of Geology and Geophysics, Chinese Academy of Sciences, Beijing 100029, People's Republic of China
Received 2020 November 23; revised 2021 March 12; accepted 2021 March 16; published 2021 April 9

Abstract

The field-aligned anisotropy of the solar wind turbulence, which is quantified by the ratio of the parallel to the perpendicular correlation (and Taylor) length scales, is determined by simultaneous two-point correlation measurements during the time period 2001–2017. Our results show that the correlation scale along the magnetic field is the largest, and the correlation scale in the field-perpendicular directions is the smallest, at both solar maximum and solar minimum. However, the Taylor scale reveals inconsistent results for different stages of the solar cycles. During the years 2001–2004, the Taylor scales are slightly larger in the field-parallel directions, while during the years 2004–2017, the Taylor scales are larger in the field-perpendicular directions. The correlation coefficient between the sunspot number and the anisotropy ratio is employed to describe the effects of solar activity on the anisotropy of solar wind turbulence. The results show that the correlation coefficient regarding the Taylor scale anisotropy (0.65) is larger than that regarding the correlation scale anisotropy (0.43), which indicates that the Taylor scale anisotropy is more sensitive to the solar activity. The Taylor scale and the correlation scale are used to calculate the effective magnetic Reynolds number, which is found to be systematically larger in the field-parallel directions than in the field-perpendicular directions. The correlation coefficient between the sunspot number and the magnetic Reynolds number anisotropy ratio is −0.75. Our results will be meaningful for understanding the solar wind turbulence anisotropy and its long-term variability in the context of solar activity.

Unified Astronomy Thesaurus concepts: Solar wind (1534); Interplanetary turbulence (830); Magnetohydrodynamics (1964); Space plasmas (1544); Solar activity (1475); Solar cycle (1487); Sunspots (1653)

1. Introduction

Plasma turbulence is a common phenomenon occurring in nature, and the turbulence in the heliosphere plays a significant role in several aspects of space plasma behaviors, such as high-energy particle acceleration, solar wind generation, plasma heating, galactic cosmic-ray modulation, and solar energetic particle propagation (Kraichnan 1965; Belcher 1971; Matthaeus & Goldstein 1982a, 1982b; Tu & Marsch 1995; Chen 2016; He & Wan 2019). Recently, the anisotropy has become one of the important aspects of the investigations of the solar wind, especially of the solar wind turbulence (e.g., Horbury et al. 2012). The turbulence anisotropy may affect the acceleration and transport of energetic particles, the heating of plasmas, and the propagation of cosmic rays in the heliosphere (Jokipii 1968a, 1968b; Jokipii & Hollweg 1970; Velli 2003; Duffy & Blundell 2005; He 2015).

One task in the field of solar wind turbulence anisotropy is to find a theoretical model for describing the turbulence anisotropy. In the solar wind observations, there are several types of fluctuation anisotropy, e.g., variance anisotropy, energy transfer rate anisotropy, power anisotropy, and correlation anisotropy (also known as spectral anisotropy or wavevector anisotropy). Of most interest is the correlation anisotropy (Duffy & Blundell 2005; Osman & Horbury 2007). At present, there exist three models for the correlation anisotropy, i.e., the "slab" model, the two-dimensional (2D) model, and the slab+2D composite model. According to the slab model, the correlation function decays in the directions parallel to the mean magnetic field, but without field-perpendicular variations. This means that the correlation function has the shortest scales in the directions parallel to the mean magnetic field and the longest scales in the field-perpendicular directions. In contrast, the 2D model considers that the correlation function decays only in the directions perpendicular to the mean magnetic field. The slab+2D two-component model was proposed by Matthaeus et al. (1990). They found that the turbulence is not consistent with either the slab model or the 2D model, but shows a "Maltese cross" shape. Therefore, they used a superposition of the slab model and the 2D model to interpret this phenomenon. Bieber et al. (1996) took the ratio of the perpendicular to quasi-parallel power spectra to quantify the anisotropy of the turbulence, and showed that near 80% of the energy is in the 2D component and 20% in the slab component. Further, Dasso et al. (2005) found that in the fast solar wind and at the larger scale of the inertial range, the correlation scales are longer in the field-perpendicular directions than in the field-parallel direction (slab model), whereas for the slow solar wind situation, the 2D component is predominant. Later, a similar result was obtained by Weygand et al. (2011). Despite that the two-component model is a rather idealized model with drastic approximation, it

Original content from this work may be used under the terms of the Creative Commons Attribution 4.0 licence. Any further distribution of this work must maintain attribution to the author(s) and the title of the work, journal citation and DOI.

can present the dominant properties of the solar wind turbulence and provide a useful parameterization for the anisotropy studies (Matthaeus et al. 1990; Bieber et al. 1996; Dasso et al. 2005; Oughton & Matthaeus 2005; Osman & Horbury 2007; Weygand et al. 2009, 2011; Horbury et al. 2012).

In most studies, a consensus conclusion can be found: the correlation length scales of the turbulent eddies in the directions parallel to the local mean magnetic field $\boldsymbol{B}_0$ are much larger than those in the directions perpendicular to $\boldsymbol{B}_0$. This indicates that the anisotropy of the correlation length scales is dominated by the 2D model. However, this is not the case for the dissipation scales. As the energy cascade proceeds to smaller scales, and reaches the plasma microscales, such as ion cyclotron (inertial) scales, electron cyclotron (inertial) scales, and possibly even smaller scales, the dissipation and heating processes are usually thought to take place. At dissipation scales, the observations of correlation anisotropy appear to be a little confusing (Chen 2016). On one hand, Weygand et al. (2009) found that the Taylor scale, which is related to the dissipation scale (Tennekes & Lumley 1972; Weygand et al. 2005), is independent of the directions relative to the mean magnetic field. On the other hand, some studies showed that the slab component dominates the anisotropy near the dissipation scales (Hamilton et al. 2008; Tessein et al. 2011; Smith et al. 2012), while others argued that the 2D component remains dominant (Chen et al. 2010; Sahraoui et al. 2010; Narita et al. 2011; Comişel et al. 2014; Perschke et al. 2014). Podesta (2009) also pointed out that the anisotropy near dissipation scales exhibits an even more complex behavior. The reason leading to this phenomenon might be that different studies may use different techniques, and the distinct scale ranges can influence the results as well. Another possible reason, which will be tested in this work, is that the Taylor scale is apt to be affected by the solar wind conditions in the context of long-term variations.

Most of the previous work has been done with single-spacecraft measurements and the frozen-in flow assumption was usually used when the mean velocity was supersonic and super-Alfvénic (Matthaeus et al. 1990; Bieber et al. 1996; Oughton & Matthaeus 2005; Osman & Horbury 2007). This situation has to some degree been improved in recent years due to the increasing exploration missions in the near-Earth solar wind. Multispacecraft analyses that can directly characterize the turbulence anisotropy without invoking the frozen-in approximation have achieved significant progress by employing modern techniques such as simultaneous two-point correlation functions (Matthaeus et al. 2005). In this work, we examine the correlation anisotropy in the solar wind fluctuations during 2001 January to 2017 December, which covers an entire solar cycle. The effects of solar activity on the turbulence anisotropy are investigated. As usual, the anisotropy is quantified by the ratio of the field-perpendicular to the field-parallel correlation (Taylor) length scales. This Letter is structured as follows. In Section 2, we provide a detailed description of the method and procedure of the two-point measurements. In Section 3, we calculate the correlation (Taylor) length scale in each angular bin during different time ranges, and discuss how the solar activity influence the anisotropy of the space plasma turbulence. A summary of our results will be provided in Section 4.

2. Methods and Procedure

In the simple scenario of homogeneous turbulence, the means, variances, and correlation values of the fluctuations should be independent of the choice of the coordinate system origin (Batchelor 1953; Tennekes & Lumley 1972; Barnes 1979; Batchelor 2000). For a magnetic field $\boldsymbol{B}(\boldsymbol{x}, t) = \boldsymbol{B}_0 + \boldsymbol{b}$, the mean is $\langle \boldsymbol{B} \rangle = \boldsymbol{B}_0$, the fluctuation is $\boldsymbol{b} = \boldsymbol{B} - \boldsymbol{B}_0$, and the variance is $\sigma^2 = \langle |\boldsymbol{b}|^2 \rangle$. The two-point correlation coefficient is

$$R(\boldsymbol{r}) = \frac{1}{\sigma^2} \langle \boldsymbol{b}(\boldsymbol{x}) \cdot \boldsymbol{b}(\boldsymbol{x} + \boldsymbol{r}) \rangle. \quad (1)$$

Here $\boldsymbol{r}$ is the separation between the two points $\boldsymbol{x}$ and $\boldsymbol{x} + \boldsymbol{r}$. For homogeneity, R and $\boldsymbol{B}_0$ are independent of $\boldsymbol{x}$. The $\langle ... \rangle$ denotes an ensemble average, which is determined by a suitably chosen time-averaging procedure. The direction-averaged correlation scale is defined as (Matthaeus et al. 2005)

$$L = \int_0^\infty R(r) dr. \quad (2)$$

Therefore, an ansatz function form of $R(r)$ can be derived from Equation (2) as $R(r) \sim e^{-r/L}$; thus, $R(r) = 1$ for $r = 0$ and $R \to 0$ for $r \to \infty$. Similarly, the Taylor scale λ can be determined from $R(r)$ as well. The Taylor scale is the length scale associated with the second-order expansion of the two-point correlation function $R(r)$ evaluated at zero separation. That is to say, the Taylor scale is the radius of curvature of the correlation function at the origin, and can be obtained from the expression $R(r) \sim 1 - (r/\sqrt{2}\lambda)^2$ (for more details, see Matthaeus et al. 2005 and Weygand et al. 2007). With these definitions, the effective magnetic Reynolds number can be obtained from the following expression:

$$R_m^{\rm eff} = \left(\frac{L}{\lambda} \right)^2. \quad (3)$$

The magnetic field data used in this investigation were measured by the triaxial fluxgate magnetometers on board spacecraft Advanced Composition Explorer (ACE), Wind, and Cluster during the time period from 2001 January to 2017 December. In our previous work, we have presented the procedures for determining $R(r)$, L, λ, and $R_m^{\rm eff}$ from multi-spacecraft data, and have shown some novel results of these scales during an entire solar cycle (Zhou et al. 2020). In this work, we use sufficient samples to resolve the correlations into angular bins that deviate from the direction parallel to the mean magnetic field, and further investigate the relationship between the correlation anisotropy and the solar activity.

In the analyses, we interpolate the spacecraft data (ACE-Wind and Cluster) to 1 minute resolution to obtain the field vectors at different positions. Note that the Cluster's orbit was in proximity to the magnetosphere. Therefore, the foreshock waves were sometimes present in the solar wind measurements. To reduce the influences of the foreshock waves, in our investigations the magnetic field measurements from the Cluster spacecraft in the solar wind are averaged to 1 minute resolution, which is much longer than the longest period for ion foreshock waves (approximately 30 s). Similar procedure for processing Cluster data was adopted by Weygand et al. (2007, 2011). The individual correlation estimates from the ACE-Wind data are computed by averaging over 24 hr

contiguous intervals of measurements. However, the correlation estimates from the Cluster data are calculated by averaging over 2 hr intervals of measurements, since the Cluster spacecraft do not remain in the solar wind for long periods. The entire data set during 2001–2017 is divided into fifteen 3 yr time periods (2001–2003, 2002–2004, …, 2014–2016, 2015–2017). In each 3 yr time period, the data intervals (approximately five hundred 24 hr intervals for ACE-Wind data and one thousand 2 hr intervals for Cluster data) are randomly selected for calculating the correlation scales and the Taylor scales. For a detailed description of the technical procedures, we refer the reader to our previous work of Zhou et al. (2020). In each data interval, we calculate the mean magnetic field by averaging the magnetic field vector over the entirety of the data interval, and further compute the magnetic field vector's time-averaged two-point correlation coefficients. This value is assigned to the time-averaged separation distance between the corresponding two spacecraft in the corresponding interval. We then determine the average value of these separation values along the field-parallel directions (x-axis) and the field-perpendicular directions (y-axis) with respect to the mean magnetic field, and assign it into the angular bin. Every angular bin is 10° wide except the bin near the field-parallel direction, which is set to be 30° wide (due to the consideration of the fewer intervals close to the parallel direction of the mean magnetic field). This angular division scheme is adopted from Weygand et al. (2009, 2011). We note that using width of 20° or 10° for the angular bin near the field-parallel direction will not qualitatively affect the obtained values for the correlation scales. Nevertheless, using the width of 20° or 10° for the angular bin near the field-parallel direction will lead to some negative (invalid) values of the obtained Taylor scales therein, due to the limited valid data in the angular bin. Therefore, we decide to use the width of 30° for the first bin (near the field-parallel direction), as in Weygand et al. (2009, 2011).

As an example, the top panel of Figure 1 shows the distribution of the data of the separation distances in the directions parallel to and perpendicular to the mean magnetic field during the divided time period 2005–2007, and the bottom panel of Figure 1 displays the corresponding plot of the correlation function contour. As we can see, the values of the correlation coefficients vary more sharply in the field-perpendicular directions than in the field-parallel directions, which indicates that the correlation length scales are the largest along the mean magnetic field and the smallest in the field-perpendicular directions (approximately 2D-dominant). The ratio of the field-parallel to the field-perpendicular correlation length scales is 1.63, which is similar to the result of 1.79 ± 0.36 proposed by Osman & Horbury (2007).

We obtain all the values of the correlation scale and the Taylor scale in different angular bins during each divided time period, and calculate the ratio of the field-parallel to the field-perpendicular values. In this work, we use the sunspot number as the indicator of the solar activity and solar cycle (Parker 1979; Hathaway 2010). Then we can investigate the solar-cycle variability of the anisotropy of the solar wind turbulence.

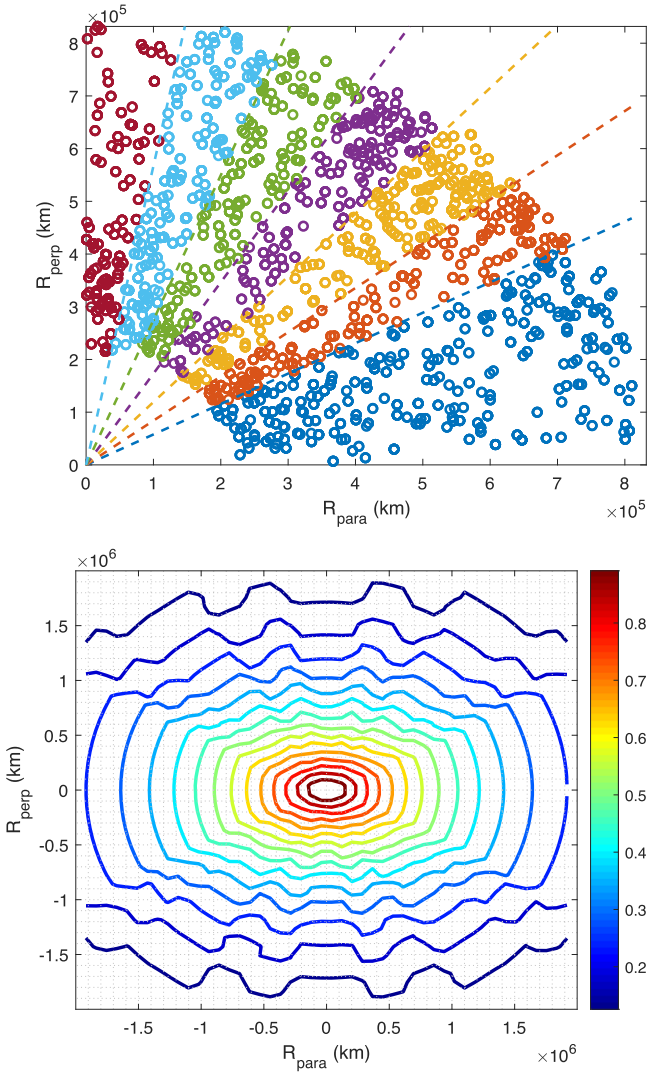

Figure 1. Top: distribution of the spacecraft separation distances in the field-parallel and field-perpendicular directions during the years 2005–2007. The dashed lines denote the boundaries of the angular bins, and the circles denote the spacecraft separations within the corresponding angular bins. Bottom: contour plot for the correlation function during the time period 2005–2007. The color scale bar denotes the values of the corresponding correlation coefficients.

3. Results and Discussion

3.1. Results

The top panel of Figure 2 shows the distribution of the correlation length scales in different angular bins during the time period 2001–2017. The values of the correlation length scale are determined from the robust fittings of the correlation function with the exponential form as discussed in Section 2. As one can see, the correlation length scale decreases systematically from the field-parallel to the field-perpendicular directions. Based on these data, we further determine the ratio of the parallel to the perpendicular correlation scales in each divided time period, and calculate the smoothed results with the Gaussian smoothing method for reducing the impact of extreme values. The bottom panel of Figure 2 reveals the evolution of the sunspot number and the ratio of the parallel to the perpendicular correlation scales. The minimum ratio of the parallel to the perpendicular correlation scales is 1.33, and the maximum ratio is 1.70. The mean value of all the correlation

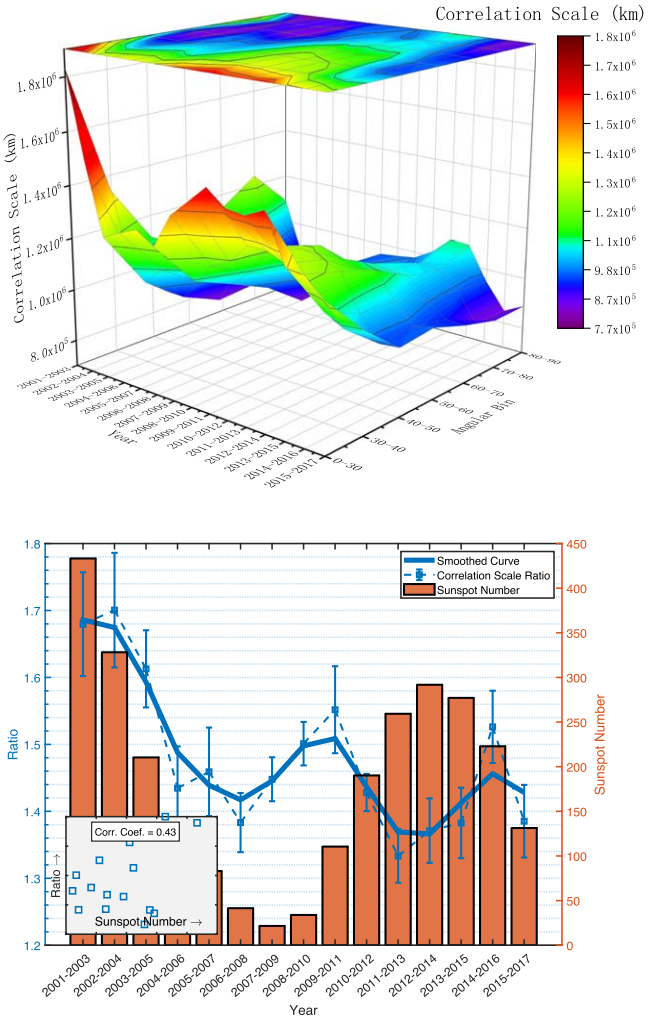

Figure 2. Top: distribution of the correlation length scales in different angular bins during the time period 2001–2017. The color scale bar on the right shows the values of the correlation scales. Bottom: evolution of the sunspot number and the ratios of the parallel to the perpendicular correlation scales during the period 2001–2017. The squares denote the ratios of the correlation scales, and the blue curve denotes the smoothed results of the ratios. The red histogram denotes the sunspot number in the divided time ranges. The inset shows the variations of the ratios of the correlation scales with the increase of the sunspot number. The correlation coefficient between the sunspot number and the anisotropy ratios of the correlation scales is 0.43.

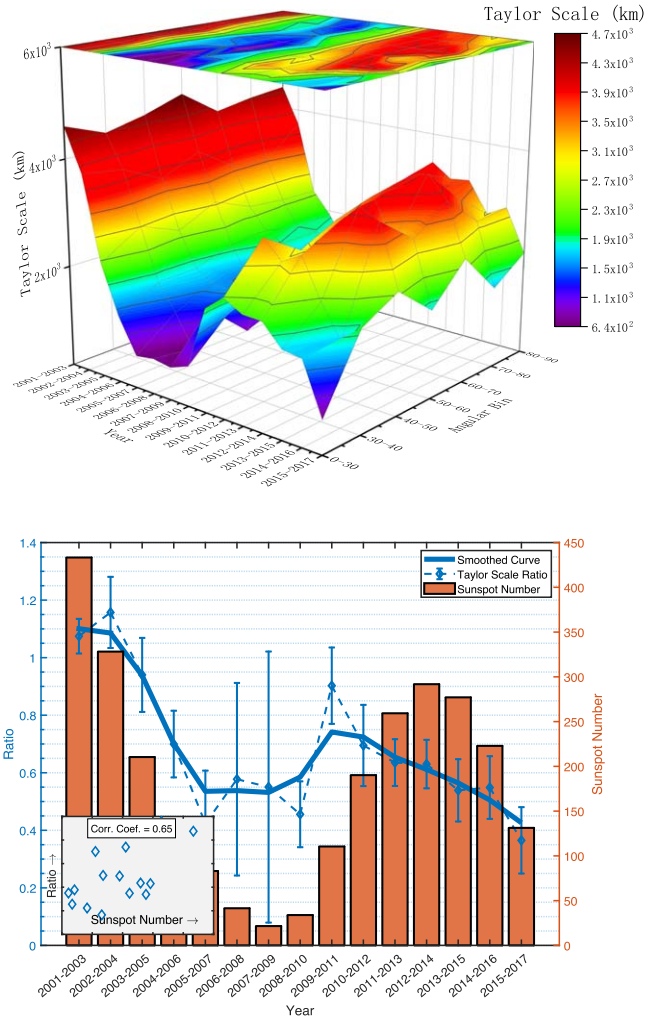

Figure 3. Top: distribution of the Taylor length scales in different angular bins during the time period 2001–2017. The color scale bar on the right shows the values of the Taylor scales. Bottom: evolution of the sunspot number and the ratios of the parallel to the perpendicular Taylor scales during the period 2001–2017. The diamonds denote the ratios of the Taylor scales, and the blue curve denotes the smoothed results of the ratios. The red histogram denotes the sunspot number in the divided time ranges. The inset shows the variations of the ratios of the Taylor scales with the increase of the sunspot number. The correlation coefficient between the sunspot number and the anisotropy ratios of the Taylor scales is 0.65.

scale ratios is 1.48, which is similar to the results provided in Dasso et al. (2005) and Osman & Horbury (2007). As we can see, all the correlation scale ratios are larger than 1. This result indicates that in the solar wind turbulence, the correlation length scale is anisotropic, and the 2D component is dominant. The correlation coefficient between the sunspot number and the anisotropy ratio of the correlation scale is 0.43, which suggests that there exists a moderately positive correlation between the solar activity and the anisotropy of the correlation length scales. Therefore, the influence of the solar activity on the anisotropy of the correlation length scales is moderate.

The top panel of Figure 3 displays the distribution of the Taylor length scales. The values of the Taylor length scale in each angular bin and during every divided time period are determined from the Richardson extrapolation method discussed in Weygand et al. (2007). Dissimilar to the correlation length scales shown in Figure 2, the Taylor length scales present more complex variations across the different angular bins. During the years 2001–2004, the Taylor length scales along the mean magnetic field are slightly larger than those along the field-perpendicular directions. During the years 2004–2017, however, the Taylor length scales are larger in the field-perpendicular directions. In addition, the Taylor length scales in the 40°–70° angular bins seem to be relatively larger. In general, the three-dimensional (3D) diagram of the Taylor length scales displays a "double-peak structure" in some divided time periods. Based on these data, we can determine the ratio of the parallel to the perpendicular Taylor length scales, and can calculate the smoothed results with the Gaussian smoothing method. The bottom panel of Figure 3 presents the evolution of the sunspot number and the ratio of the parallel to the perpendicular Taylor length scales. The minimum of the ratios of the parallel to the perpendicular Taylor scales is 0.37, and the maximum is 1.16. The averaged value of all the Taylor scale ratios is 0.68, which is similar to the result 0.91 ± 0.45 implied in Weygand et al. (2009). As

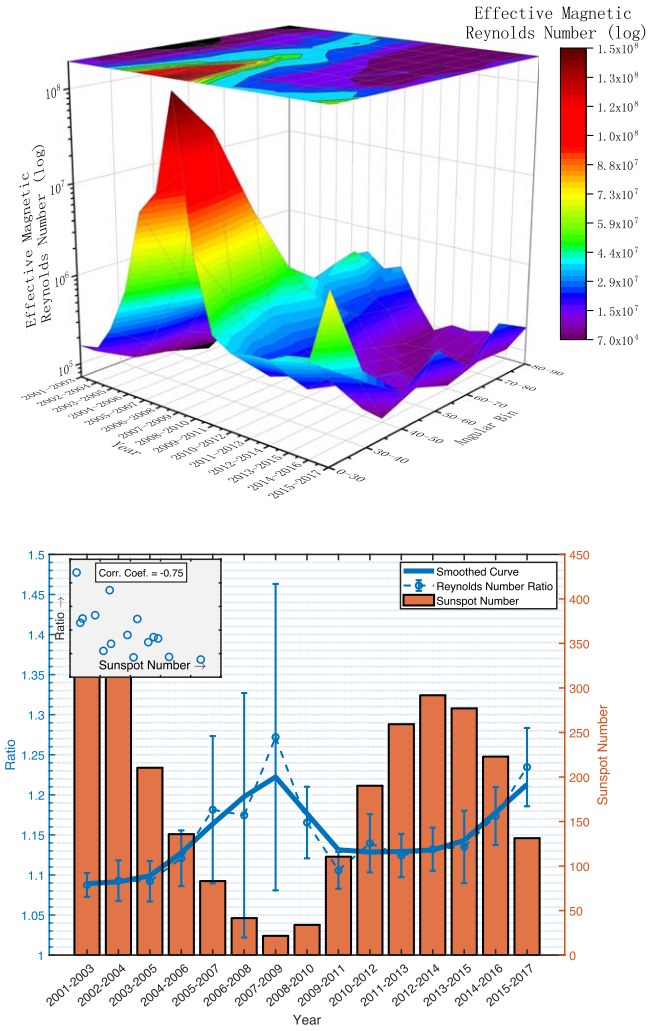

Figure 4. Top: distribution of the effective magnetic Reynolds number (in logarithmic unit) in different angular bins during the time period 2001–2017. The color scale bar on the right shows the values of the effective magnetic Reynolds number in logarithmic unit. Bottom: evolution of the sunspot number and the ratios of the parallel to the perpendicular effective magnetic Reynolds number (logarithmic unit) during the period 2001–2017. The circles denote the ratios of the effective magnetic Reynolds number, and the blue curve denotes smoothed results of the ratios. The red histogram denotes the sunspot number in the divided time ranges. The inset displays the variations of the ratios of the effective magnetic Reynolds number with the increase of the sunspot number. The correlation coefficient between the sunspot number and the anisotropy ratios of the effective magnetic Reynolds number is −0.75.

shown, most of the Taylor scale ratios are smaller than 1, which indicates that in the solar wind turbulence, the Taylor length scale is generally anisotropic, and the slab component is dominant. The correlation coefficient between the sunspot number and the anisotropy ratio of the Taylor scale is 0.65. This result suggests that there exists a relatively strong positive correlation between the solar activity and the anisotropy of the Taylor length scales.

The top panel of Figure 4 presents the distribution of the effective magnetic Reynolds number. The values of the effective magnetic Reynolds number in each angular bin and during each divided time period are calculated by using Equation (3). As shown in the previous results of Zhou et al. (2020), the effective magnetic Reynolds number is closely related with the solar activity. During the period 2001–2017, the minimum and maximum values of the effective magnetic Reynolds number are 96,467.7 and 692,071.1, respectively, and the averaged value of the effective magnetic Reynolds number is 302,827.4 (Zhou et al. 2020). For a clearer illustration, here we use a logarithmic unit in presenting the results of the effective magnetic Reynolds number. As one can see, the effective magnetic Reynolds number in the field-parallel directions is systematically larger than that in the field-perpendicular directions, which means that the 2D component is approximately dominant. The bottom panel of Figure 4 shows the evolution of the sunspot number and the ratio of the parallel to the perpendicular effective magnetic Reynolds number during the years 2001–2017. The minimum and maximum ratios of the parallel to the perpendicular effective magnetic Reynolds numbers are 1.09 and 1.27, respectively, and the mean value of all the ratios of the effective magnetic Reynolds number is 1.15, which is quite similar to the values of ∼1.14 computed from the results presented in Weygand et al. (2009). The correlation coefficient between the sunspot number and the anisotropy ratio of the effective magnetic Reynolds number is −0.75, which indicates that there exists a relatively strong negative correlation between the solar activity and the anisotropy of the effective magnetic Reynolds number. That is to say, the effective magnetic Reynolds number is less anisotropic during a solar maximum.

3.2. Discussion

As shown in Figure 2, the anisotropy of the correlation length scale is only weakly affected by the solar activity, namely, the anisotropy of the correlation scale is relatively stable during the whole solar cycle. In addition, the anisotropy of the correlation length scales is dominantly controlled by the 2D component, which is consistent with the previous studies. Due to the weak dependence on the solar activity, the anisotropy values of the correlation scale investigated by different authors during different phases of solar cycles usually reveal the similar results.

Although consistent results can be found for the anisotropy of the correlation scale, this is not the case for the anisotropy of the Taylor (and/or dissipation) scale. At the Taylor and dissipation scales, the observational investigations of the correlation anisotropy usually present inconsistent results. These conflicting results in the literature can be reconciled by our findings in this work. As shown in Figure 3, the correlation coefficient between the sunspot number and the ratio of the field-parallel to the field-perpendicular Taylor length scales is 0.65, which indicates that the effects of the solar activity on the correlation anisotropy near the Taylor scales are relatively strong. Therefore, the anisotropy of the Taylor scale is relatively unstable and varies with the declining and rise activity phases of solar cycles. Specifically, the anisotropy of the Taylor scale is 2D-component dominated during the strong solar activity phases, and is slab-component dominated during the weak solar activity phases. This finding suggests that the long-term solar activity variations may significantly affect the anisotropy of the Taylor scales. In addition, the 3D diagram of the Taylor length scales in Figure 3 displays a "double-peak" structure in some divided time ranges. The Taylor length scales in the angular bins 40°–70° are relatively large. During the years 2011–2015 (solar maximum), this phenomenon is more pronounced.

The distribution of the correlation length scales does not show obvious "double-peak" structure. Instead, it displays a

Table 1
Values of Correlation Coefficients between Sunspot Number and Correlation Length Scales and Taylor Length Scales in Different Angular Bins during 2001–2017

	0°–30°	30°–40°	40°–50°	50°–60°	60°–70°	70°–80°	80°–90°
Correlation scale	0.57 ± 0.03	0.31 ± 0.11	0.04 ± 0.09	0.05 ± 0.05	0.56 ± 0.05	0.65 ± 0.05	0.34 ± 0.09
Taylor scale	0.84 ± 0.03	0.81 ± 0.05	0.91 ± 0.03	0.95 ± 0.02	0.88 ± 0.05	0.89 ± 0.03	0.90 ± 0.02

relatively small gradient in the angular bins 40°–70°, especially at the solar maximum. Combining the behaviors of the correlation scales and the Taylor scales, we can find that both these scales show some unusual properties near the angle of 50°. To specifically investigate this interesting phenomenon, we calculate the correlation coefficients between the sunspot number and both the correlation length scales and the Taylor length scales in each angular bin, and present the results in Table 1. As we can see, the values of the correlation coefficients for the correlation scales decrease when the angular bins vary from 0°–30° (approximately field-parallel) to 40°–60°. In the angular bins 40°–50° and 50°–60°, the correlation coefficients become very small (i.e., 0.04 ± 0.09 and 0.05 ± 0.05). These nearly zero values indicate that the correlation scales in these directions are not affected by the solar activity. However, the correlation coefficient in the angular bin 0°–30° (nearly field-parallel) is large (i.e., 0.57 ± 0.03). This result suggests that the correlation scale in the field-parallel direction is considerably affected by the solar activity. This finding will be useful for understanding the anisotropy of the correlation scales. For the Taylor scales, the values of the correlation coefficients generally increase when the angular bins vary from 0°–30° (nearly field-parallel) and 80°–90° (nearly field-perpendicular) to 50°–60°. Therefore, near the angular bin 50°–60°, where the value of the correlation coefficient is 0.95 ± 0.02, the Taylor scale is most easily influenced by the solar activity. We note that in all directions relative to the mean magnetic field, the solar activity significantly influences the Taylor scales. This is one manifestation of the complexity of the Taylor scale anisotropy.

In this work, we do not investigate the specific effects of fast/slow solar wind on the correlation scale anisotropy and the Taylor scale anisotropy, which is also an interesting topic in the field of solar wind turbulence and was investigated by Weygand et al. (2011). To compare with the results in Weygand et al. (2011) and other relevant works in the context of fast/slow solar wind may be the subject of our future work. In this Letter, we primarily investigate the solar-cycle variations of the anisotropy of Taylor scale and correlation scale. Note that we mainly present the experimental observation results of the solar-cycle variations of the anisotropy in the solar wind turbulence. A detailed discussion and explanation regarding the physical mechanism of this phenomenon may be one topic of our future work.

4. Summary

Based on the simultaneous two-point correlation function measurements, in this work we investigate the solar-cycle variations of the anisotropy of the correlation scales and the Taylor scales in the solar wind turbulence. The magnetic field data used in this investigation were measured by the triaxial fluxgate magnetometers on board spacecraft ACE, Wind, and Cluster during the period from 2001 January to 2017 December, which covers more than an entire solar cycle. The data accumulated over a long time are sufficient to study the effects of long-term solar activity on the anisotropy of the solar wind turbulence. Generally, the correlation scale length decreases with the relative angle between magnetic field fluctuation and the average magnetic field, independent of the solar activity. The averaged value of all the ratios of the correlation scales is 1.48, which is similar to the results presented in Dasso et al. (2005) and Osman & Horbury (2007). The correlation coefficient between the sunspot number and the anisotropy ratios of the correlation scales is 0.43, which indicates that the influence of the solar activity on the anisotropy of the correlation length scales is not so significant. Furthermore, we find that the anisotropy of the correlation scales is dominated by the 2D component. However, this is not the case for the anisotropy of the Taylor (and/or dissipation) scales. The minimum ratio of the parallel to the perpendicular Taylor scales is 0.37, and the maximum ratio is 1.16. The averaged value of all the ratios is 0.68, which is consistent with the values of 0.91 ± 0.45 calculated from the results in Weygand et al. (2009). The correlation coefficient between the sunspot number and the anisotropy ratios of the Taylor scales is 0.65, which indicates that the anisotropy of the Taylor scales is relatively significantly affected by the long-term solar activity. We further find that near/during the solar maximum, the anisotropy of the Taylor scale is 2D-component dominated, while near/during the solar minimum, the anisotropy of the Taylor scale is slab-component dominated.

Using the Taylor scales and the correlation scales, we further determine the value of the effective magnetic Reynolds number for each angular bin. We find that the effective magnetic Reynolds number in the field-parallel directions is systematically larger than that in the field-perpendicular directions, which indicates that the 2D component is dominant. The averaged value of all the ratios of the effective magnetic Reynolds number is 1.15, which agrees well with the values of $\sim$1.14 calculated from the results shown in Weygand et al. (2009). The correlation coefficient between the sunspot number and the anisotropy ratios is -0.75, which implies that there exists a relatively strong negative correlation between the solar activity and the anisotropy of the effective magnetic Reynolds number.

In addition, the correlation coefficient between the sunspot number and the Taylor length scales is systematically larger than that between the sunspot number and the correlation length scales. This result means that the Taylor scale is more easily influenced by the long-term solar activity than the correlation scale. Furthermore, the correlation scales near the field-parallel and field-perpendicular directions are most easily affected by the solar activity among all the directions. However, the Taylor scales in all directions relative to the mean magnetic field are significantly influenced by the long-term solar activity. These results will be very useful for better understanding the anisotropy of the solar wind turbulence and especially its solar-cycle variability.

This work was supported in part by the B-type Strategic Priority Program of the Chinese Academy of Sciences under grant XDB41000000, the National Natural Science Foundation of China under grants 41874207, 41621063, 41474154, and 41204130, and the Chinese Academy of Sciences under grant KZZD-EW-01-2. H.-Q.H. gratefully acknowledges the partial support of the Youth Innovation Promotion Association of the Chinese Academy of Sciences (No. 2017091). We benefited from the data of ACE, Wind, and Cluster provided by NASA/Space Physics Data Facility (SPDF)/CDAWeb. The sunspot data were provided by the World Data Center SILSO, Royal Observatory of Belgium, Brussels.

References

Barnes, A. 1979, in Solar System Plasma Physics, ed. E. N. Parker, C. F. Kennel, & L. J. Lanzerotti (Amsterdam: North-Holland Publishing Co.), 249
Batchelor, G. K. 1953, The Theory of Homogeneous Turbulence (Cambridge: Cambridge Univ. Press)
Batchelor, G. K. 2000, An Introduction to Fluid Dynamics (Cambridge: Cambridge Univ. Press)
Belcher, J. W. 1971, ApJ, 168, 509
Bieber, J. W., Wanner, W., & Matthaeus, W. H. 1996, JGR, 101, 2511
Chen, C. H. K. 2016, JPlPh, 82, 535820602
Chen, C. H. K., Horbury, T. S., Schekochihin, A. A., et al. 2010, PhRvL, 104, 255002
Comişel, H., Narita, Y., & Motschmann, U. 2014, NPGeo, 21, 1075
Dasso, S., Milano, L. J., Matthaeus, W. H., & Smith, C. W. 2005, ApJL, 635, L181
Duffy, P., & Blundell, K. M. 2005, PPCF, 47, B667
Hamilton, K., Smith, C. W., Vasquez, B. J., & Leamon, R. J. 2008, JGRA, 113, 01106
Hathaway, D. H. 2010, LRSP, 7, 1
He, H.-Q. 2015, ApJ, 814, 157
He, H.-Q., & Wan, W. 2019, ApJL, 885, L28
Horbury, T. S., Wicks, R. T., & Chen, C. H. K. 2012, SSRv, 172, 325
Jokipii, J. R. 1968a, ApJ, 152, 799
Jokipii, J. R. 1968b, ApJ, 152, 997
Jokipii, J. R., & Hollweg, J. V. 1970, ApJ, 160, 745
Kraichnan, R. H. 1965, PhFl, 8, 1385
Matthaeus, W. H., Dasso, S., Weygand, J. M., et al. 2005, PhRvL, 95, 231101
Matthaeus, W. H., & Goldstein, M. L. 1982a, JGR, 87, 6011
Matthaeus, W. H., & Goldstein, M. L. 1982b, JGR, 87, 10347
Matthaeus, W. H., Goldstein, M. L., & Roberts, D. A. 1990, JGR, 95, 20673
Narita, Y., Gary, S. P., Saito, S., Glassmeier, K. H., & Motschmann, U. 2011, GeoRL, 38, L05101
Osman, K. T., & Horbury, T. S. 2007, ApJL, 654, L103
Oughton, S., & Matthaeus, W. H. 2005, NPGeo, 12, 299
Parker, E. N. 1979, Cosmical Magnetic Fields: Their Origin and Their Activity (Oxford, New York: Clarendon, Oxford Univ. Press)
Perschke, C., Narita, Y., Motschmann, U., & Glassmeier, K.-H. 2014, ApJL, 793, L25
Podesta, J. J. 2009, ApJ, 698, 986
Sahraoui, F., Goldstein, M. L., Belmont, G., Canu, P., & Rezeau, L. 2010, PhRvL, 105, 131101
Smith, C. W., Vasquez, B. J., & Hollweg, J. V. 2012, ApJ, 745, 8
Tennekes, H., & Lumley, J. L. 1972, First Course in Turbulence (Cambridge, MA: MIT Press)
Tessein, J. A., Smith, C. W., Vasquez, B. J., & Skoug, R. M. 2011, JGRA, 116, 10103
Tu, C.-Y., & Marsch, E. 1995, SSRv, 73, 1
Velli, M. 2003, PPCF, 45, A205
Weygand, J. M., Kivelson, M. G., Khurana, K. K., et al. 2005, JGRA, 110, 01205
Weygand, J. M., Matthaeus, W. H., Dasso, S., et al. 2009, JGRA, 114, 07213
Weygand, J. M., Matthaeus, W. H., Dasso, S., & Kivelson, M. G. 2011, JGRA, 116, 08102
Weygand, J. M., Matthaeus, W. H., Dasso, S., Kivelson, M. G., & Walker, R. J. 2007, JGRA, 112, 10201
Zhou, G., He, H.-Q., & Wan, W. 2020, ApJL, 899, L32